

Oct 28, 2020

# 🌐 Atomic Force Microscopy of DNA and DNA-Protein Interactions

📁 In 1 collection

DOI

[dx.doi.org/10.17504/protocols.io.bncemate](https://dx.doi.org/10.17504/protocols.io.bncemate)

Philip J. Haynes<sup>1,2,3</sup>, Kavita H. S. Main<sup>1,4</sup>, Alice L Pyne<sup>5</sup>

<sup>1</sup>London Centre for Nanotechnology, University College London, London WC1H 0AH, UK;

<sup>2</sup>Molecular Science Research Hub, Department of Chemistry, Imperial College London, W12 0BZ, UK;

<sup>3</sup>Department of Physics and Astronomy, University College London, London, WC1E 6BT, UK;

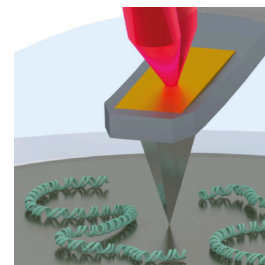
<sup>4</sup>UCL Cancer Institute, University College London, London, WC1E 6DD, UK;

<sup>5</sup>Department of Materials Science, Sir Robert Hadfield Building, University of Sheffield, S1 3JD



**Alice L Pyne**

Department of Materials Science, Sir Robert Hadfield Buildin...



OPEN  ACCESS



DOI: [dx.doi.org/10.17504/protocols.io.bncemate](https://dx.doi.org/10.17504/protocols.io.bncemate)

**Collection Citation:** Philip J. Haynes, Kavita H. S. Main, Alice L Pyne 2020. Atomic Force Microscopy of DNA and DNA-Protein Interactions. **protocols.io** <https://dx.doi.org/10.17504/protocols.io.bncemate>

**Manuscript citation:**

Base-pair resolution analysis of the effect of supercoiling on DNA flexibility and major groove recognition by triplex-forming oligonucleotides

**License:** This is an open access collection distributed under the terms of the **Creative Commons Attribution License**, which permits unrestricted use, distribution, and reproduction in any medium, provided the original author and source are credited

**Protocol status:** Working

**We use this protocol and it's working**

**Created:** October 13, 2020

**Last Modified:** October 28, 2020

**Collection Integer ID:** 43110

**Keywords:** Atomic force microscopy, AFM, DNA, Supercoiling, Double helix, DNA-protein binding,

## Abstract

Atomic force microscopy (AFM) is a microscopy technique that uses a sharp probe to trace a sample surface at nanometre resolution. For biological applications, one of its key advantages is its ability to visualize substructure of single molecules and molecular complexes in an aqueous environment. Here, we describe the application of AFM to determine the secondary and tertiary structure of surface-bound DNA, and its interactions with proteins.

## Methods:

Mica and DNA are both negatively charged at a neutral pH in aqueous solution. There are a number of methods used to facilitate the adsorption of DNA to the mica surface [9, 24, 29-31]. The following sections describe three methods to facilitate DNA and DNA-protein adsorption on mica, which are appropriate for imaging DNA in liquid (see **Note 5**).

Mica substrates can be attached to a steel disc to be mounted on magnetic sample holders as common in AFM instruments (see **Note 6**).

## Attachments



Imaging\_DNA\_by\_AFM

P...

2.5MB

## Guidelines

### Running Head

#### Atomic Force Microscopy of DNA and DNA-Protein Interactions

### Introduction

Atomic force microscopy (AFM, see Fig. 1) is a unique tool to obtain structural information of single biomolecules at ~1 nm spatial resolution. AFM allows for characterization of molecules adsorbed on a planar substrate in aqueous solution, *i.e.*, without the need for chemical fixation, staining, or vitrifying (Fig 1). AFM can be performed in air or in fluid. In-air AFM is more straightforward in operation and can provide static snapshots of reactions that involve DNA in solution (*i.e.* taking place while the DNA was free in solution and not bound to the planar substrate) by drying the sample before imaging. However, AFM in liquid has both yielded the highest spatial resolution on DNA [1-3], and can also be used to observe biomolecular dynamics [4-6]. AFM has been extensively used to visualize DNA supercoiling [7-11], non-canonical DNA secondary structures [11-12], DNA origami assemblies [13-14], interactions with therapeutic agents [15-16] and DNA-protein complexes [17-22], with the additional advantage that binding events and conformational changes can be monitored in real time [5-6, 21]. AFM can discern the helical pitch of DNA [23-27] and RNA [28], and under appropriate imaging conditions, resolve the two strands of the DNA double helix (Fig. 2a) [1-3].

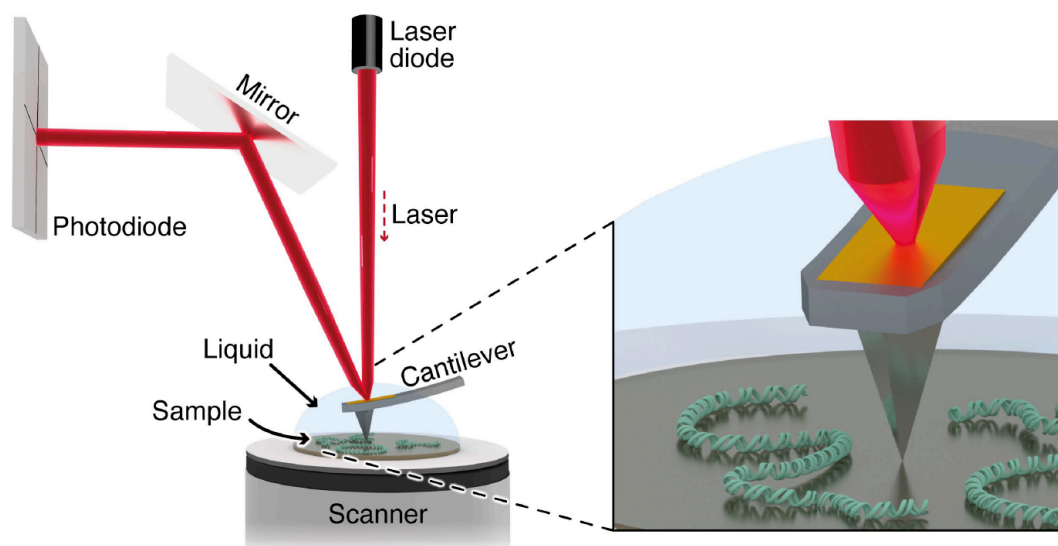


**Fig. 1** Schematic of AFM in aqueous solution. A sharp tip is scanned line-by-line across the sample surface to build up an image of the surface topography. The topography at each scanned point is a function of the tip-sample interaction which is monitored by measuring the bending of the cantilever to which the tip is attached. The bending of the cantilever is usually detected via a laser beam deflected on a position-sensitive detector (4-quadrant photodiode). The sample is mounted on a (usually piezoelectric) scanner for three-dimensional positioning with sub-nanometer accuracy. The sample, the tip and the cantilever are immersed in liquid. *Inset:* magnified for clarity.

For high-resolution AFM imaging, the sample must be adsorbed onto an atomically flat substrate, such that observed topographic features can be attributed to the biological sample and not to the substrate. Muscovite mica is often used as a substrate for AFM imaging, since its structure consists of many weakly interacting planes. These planes can be cleaved using sticky tape, resulting in an atomically flat surface. The disadvantage of mica

as a substrate for DNA imaging is that both mica and DNA are negatively charged at neutral pH in aqueous solution, impeding the adsorption of DNA to the mica. Various methods that modify the surface charge of mica have been developed to facilitate DNA adsorption. These include: functionalizing the mica with aminopropyltriethoxy silane (APTES) or aminopropyl silatrane (APS) to create a positively charged surface [29]; using monovalent and divalent cations to bridge the charge repulsion [30]; adsorbing a positively charged lipid bilayer to the mica to facilitate electrostatically driven adsorption [24]; and functionalization with polymers (*e.g.*, poly-L-lysine) to create a positively charged monolayer on the surface [9]. Here we cover the divalent cation method and the use of poly-L-lysine based mica functionalizations which facilitate high resolution imaging of DNA. This allows for structural insights into variations in DNA structure at both a local and global level, at a resolution where the both the minor and major grooves can be resolved (Fig. 2a).

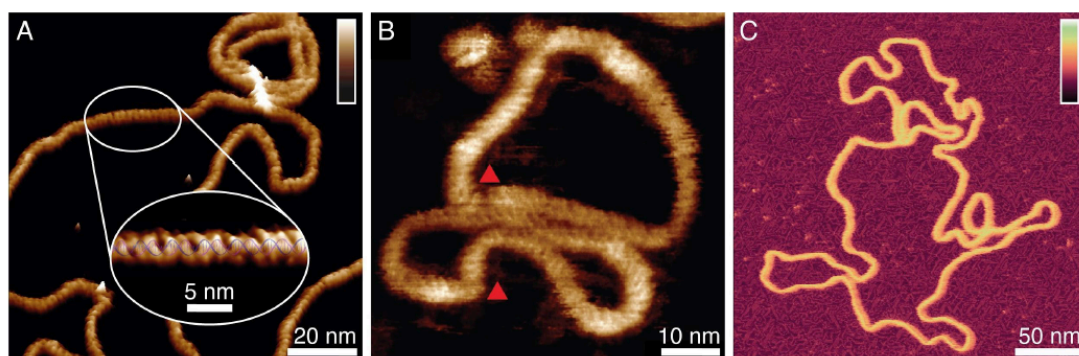


**Fig. 2** High-resolution topographic images of DNA acquired by PeakForce Tapping mode (protocol 4.). The divalent cation method (**protocol 2, method 2.1**) is used to adsorb **(a)** DNA plasmids and **(b)** 339 base-pair DNA minicircles. In **a**, the two strands of the DNA double-helix are captured. *Inset*: a higher resolution image digitally straightened and overlaid with a cartoon representation of the B-DNA crystal structure. Color scales: 2.5 nm (main), 1.2 nm (*inset*). In **b**, defects and disruptions in the canonical B-form DNA are observed (red triangles), as a step-change in the angle of the helix. Color scale (scale bar in **a**): 2.5 nm [ref. 11, with permission]. **(c)** A DNA plasmid adsorbed onto PLL<sub>1000–2000</sub>-functionalized mica (**protocol 2, method 2.3**) where the chains of poly-L-lysine making up the underlying substrate are resolved. Colour scale: 8 nm [adapted from ref. 31, with permission].

In typical AFM experiments, the sample preparation is a compromise between the need to immobilize the DNA for high spatial resolution and, for real-time imaging of binding events and conformational changes, the need to allow DNA sufficient freedom for structural rearrangements. In addition, when using salts to facilitate DNA adsorption on a substrate, there is -- in particular for the commonly used  $\text{NiCl}_2$  -- the possibility of salt accumulation on the substrate, which may compromise the resolution and interpretation of the resulting AFM images [1–3]. The poly-L-lysine preparation has the advantage of not requiring particular salts in the solution. However, due to its gross positive charge and adhesiveness, it may bring in other contaminants from the solution.

This is further exacerbated when interrogating DNA-protein interactions, as nonspecific protein binding to the underlying substrate is problematic at biologically relevant protein concentrations. At these concentrations, non-specifically bound protein obscures the specifically adsorbed DNA-bound protein complexes (**protocol 5**). This non-specific binding is further amplified when the DNA-protein affinity is considered low and higher concentrations of protein are required to observe binding. To curtail this, the surface can be PEGylated using diblock copolymers that contain poly-L-lysine (surface binding domain) and polyethylene glycol (surface

passivating domain) [31]. The addition of poly(L-lysine)-*b*-poly(ethylene glycol) (PLL-*b*-PEG) achieves selective DNA adsorption whilst minimising non-specific protein adsorption, where PEG suppresses protein binding by steric repulsion.

In addition to sample preparation, a critical element for high resolution AFM imaging is force sensitivity and control [1-3]. Generally, the AFM probe needs to exert a force on the sample to be able to record the surface topography. However if this force is too large, it can cause sample deformation or contamination of the probe, both of which can reduce the resolution of the resulting image. To minimise the force exerted on the sample, a wide range of operational modes have been developed. The best high-resolution AFM images in the literature appear highly similar. This illustrates that there is more than one route to high-resolution imaging given that all required parameters are optimized, however, these modes vary in the ease by which the imaging is achieved. In particular, early DNA double helix imaging was carried out using phase and frequency modulation techniques, which typically achieve high sensitivity using stiffer cantilevers [1-2].

Here, we describe a widely implemented method for in-liquid AFM imaging of DNA that has been successfully employed to visualize the DNA double helix: rapid forcedistance imaging mode (also called Force Modulation or PeakForce™ Tapping mode, see Fig. 3). Rapid force-distance AFM minimises the tip-sample interaction by measuring the force applied by the tip to the sample at each point during imaging/scanning. It does so by taking repeated force curves across the sample whereby the tip is approached to and retracted from the surface. As the tip interacts with the surface the applied force is measured with respect to the baseline away from the surface, for each force curve (Fig. 3b). By measuring the height at which the force reaches a predefined setpoint, we can determine the sample topography at each interaction point, thereby modulating the vertical tip-sample distance.

The surface preparations described below are not limited to rapid force-distance imaging (PeakForce Tapping) and the AFM system of choice. Our description presumes some knowledge about elementary AFM operation, such as can be found in instrument manuals.

## Notes

1. The cantilever resonance in fluid is around three times less than that quoted in air by the manufacturer.
2. Prepare all solutions using ultrapure water *e.g.* MilliQ®, which is prepared by purifying deionized water to a resistivity > 18 MΩ and TOC < 10 ppb at 25 °C) and using analytical-grade reagents.
3. Any imaging buffer can be used with the poly-L-lysine method. The addition of cations *e.g.* Na<sup>+</sup> (NaCl) and Ca<sup>2+</sup> will screen the electrostatic repulsion between the tip and the DNA which are both negatively charged in solution at physiological pH. This allows for better resolution as the tip can follow the contours of the DNA more easily. Changing the imaging buffer and concentration of cations may require different DNA deposition times. If poly-L-lysine is being used with a pH 5 imaging buffer, adding NaOAc will help combat the extra PLL-tip interactions caused by protonation of lysine residues.
4. Stocks may be stored at any concentration and diluted in the buffer to the final concentration shown.
5. All surface modifications can contaminate tips during imaging. A disadvantage of using NiCl<sub>2</sub> is that it tends to precipitate on the mica surface, with increased risk of contaminating the AFM probe. Poly-L-lysine, due to its affinity to typical AFM tips, increases the probability of tip artifacts *e.g.* double-tip.
6. Alternatively and depending on the AFM instrument, the mica disc can be glued to a glass slide.



7. A layer of (hydrophobic) PTFE (or Teflon) is placed below the mica to confine the liquid solution to the mica disc and avoid contamination and spillage when imaging in fluid.
8. If liquid is placed on the mica before the superglue is dry, the glue will form a film over the droplet which may damage the fluid cell.
9. The DNA and buffers should equilibrate to the temperature of the AFM to minimize the effect of drift. Whilst making up samples, equilibrate the AFM in a clean buffer solution and turn the laser on.
10. The strength of DNA adsorption can be tuned by altering the  $\text{NiCl}_2$  concentration in the buffer. Typically, higher  $\text{Ni}^{2+}$  concentrations lead to a stronger binding of adsorbed DNA molecules to the mica, which facilitates AFM imaging, but also results in increased surface contamination by the formation of  $\text{NiCl}_2$  salt aggregates through precipitation. The likelihood of  $\text{NiCl}_2$  precipitation increases with time.
11. Smaller mica discs can be used to reduce the amount of DNA required. Adjust the volume of solutions added to the mica (DNA, imaging buffer) accordingly.
12. The final volume depends on the system and it's fluid cell. For a 6 mm mica disc, ~40  $\mu\text{L}$  with a MultiMode<sup>®</sup> fluid cell, ~30  $\mu\text{L}$  with the FastScan Bio<sup>™</sup> AFM. A clear capillary bridge should be seen with near-straight edges.
13. The buffer may be exchanged for any imaging buffer to remove DNA that is not adsorbed. This step can be missed out if the user requires, with the caveat that material floating in solution may interfere with imaging.
14. The PLL-b-PEG block copolymer used here can be purchased as a lyophilized powder from Alamanda polymers (mPEG5k-b-PLKC10, methoxy-poly(ethylene glycol)-block-poly(L-lysine hydrochloride). Store the powder at -20 °C in ~1 mg powder aliquots. On the day of use/imaging, dissolve a powder aliquot to 1 mg/mL in ultrapure water. A liquid aliquot should keep at 4°C for ~1 week.
15. Care must be taken to ensure that the surface is kept hydrated at all times. Keep samples under humidity in a petri dish during incubation (lid covered, damp tissue placed inside) and hydrated during imaging. As a sample dries, the precipitation of salts (*e.g.*  $\text{NiCl}_2$ ) will contaminate the surface and interfere with imaging.
16. A higher concentration of DNA will need to be used when compared to PLL-only adsorption of the same sample. This is due to a combination of PEG inhibiting the approach of DNA and the reduced density of PLL on the surface.
17. When exchanging the buffer and/or protein during imaging, the use of microcapillary gel pipette tips can be used to minimise the required cantilever withdraw distance.
18. *Setpoints* are often measured in Volts as directly read via the detector readout of the cantilever deflection. To convert these into forces, the *Setpoint* value in Volts can be multiplied by the sensitivity of the deflection detection and the spring constant of the cantilever.
19. The cantilever resonance should be at least three times greater than the *PeakForce Frequency*. When doubling the *PeakForce Frequency* during imaging the Sync Distance should be reduced by approximately one third.
20. At low *Engage Setpoints*, using soft cantilevers, the cantilever may finish its approach before having made contact with the surface. In this case approach the cantilever again. If the approach fails repeatedly, you may need to increase the *Engage Setpoint*.
21. The *Sync Distance* parameter comes in two forms: *Sync Distance New* (diamond marker) and *Sync Distance QNM*. *Sync Distance New* controls the feedback loop. It is the time between the point of maximum force, and the maximum withdraw for each force curve. If this is incorrect the feedback will not work correctly and the tip and/or sample may be damaged. The *Sync Distance QNM* is used in the calculation of mechanical properties and is observable as the point at which the Force-Z curve 'folds' about its axis at the turnaround point. The *Sync Distance QNM* can be set as the same as *Sync Distance* for imaging only but must be calibrated to

extract mechanical properties, but plays no role in the feedback loop. When set the same as the *Sync Distance New*, the *Sync Distance QNM* can be used to check the calculation is correct by checking the Force-Z curve 'folds' at the point of maximum force.

22. The *PeakForce Amplitude* should be on the same order as the expected height features multiplied by two. This is such that the sampling of data points taken is performed when the tip is in the contact region. Reducing the amplitude reduces noise (since tip motion is reduced) and hydrodynamic drag (the higher the amplitude, the more fluid there is to push).
23. At low applied forces, the tip may not be able to track the molecule well. Even with high *Feedback Gain*, this may result in an effect known as parachuting. This is where the tip fails to quickly move back towards the surface after having moved up on contact with a protrusion such as adsorbed DNA. This can lead to streaky features extending from the molecule in the direction of scanning.
24. On reducing the *Scan Size*, the imaging setpoint may need to be reduced and the gains readjusted, as the tip now spends more time interacting with the same sample area, which can imply an increased risk of damage to the DNA molecule(s).
25. Such drift or creep may be reduced by operating the AFM with a closed-loop scanner, but may also depend on the microscope design.
26. The *Lift Height* is the distance above the surface where the background force, taking the form of hydrodynamic damping, is measured. The *Lift Height* should be larger than the molecule of interest. If the *Lift Height* is not set correctly the non-interacting region of the force curve will not appear flat, and forces may be calculated/applied incorrectly.
27. The application of higher forces will hinder access to the highest spatial resolution and the DNA may appear compressed (Fig. 4). If the DNA-protein affinity is considerably high and non-transient, then it is possible to circumvent this by tuning the extent of polymerisation (i.e. polymer length) for both the PLL and the PEG in the PLL-*b*-PEG copolymer. To increase DNA coverage, choose shorter PEG brushes and longer PLL chains. This will inherently increase non-specific protein binding to the surface. A shorter PEG chain may provide access to regimes that benefit high-resolution imaging, as well as improved DNA adsorption, with the usual caveat being the risk of non-specific protein binding. Increasing the PEG length away from the 113 units used here, DNA adsorption may be inhibited completely [31].
28. It would follow that the smaller the tip radius, the higher resolution that can be achieved, but this is not always the case. For smaller tip radii the same tipsample force is exerted on a smaller area of the sample, applying a larger pressure, and correspondingly a larger risk of sample distortion.
29. Can increase the gains to the point at which the noise in the surface topography begins to significantly increase and then reduce by up to a third.

## Acknowledgements

We would like to thank Dr Richard Thorogate, Dr Andrea Slade, Dr Shuiqing Hu, Dr Bede Pittenger, Dr Thomas Muller, and Dr Chanmin Su for advice, technical support and resources. We acknowledge funding by the UK's Department for Business, Energy and Industrial Strategy, the Engineering and Physical Sciences Research Council (EPSRC: EP/L015277/1; EP/M028100/1), the Medical Research Council (MR/ R024871/1); and the Francis Crick institute: CRUK (FC001119), MRC (FC001119) and the Wellcome Trust (FC001119).

## References


1. Leung C, Bestembayeva A, Thorogate R, Stinson J, Pyne A, Marcovich C, Yang JL, Drechsler U, Despont M, Jankowski T (2012) Atomic force microscopy with nanoscale cantilevers resolves different structural conformations of the DNA double helix. *Nano Lett* 12(7):3846–3850. doi:10.1021/nl301857p
2. Ido S, Kimura K, Oyabu N, Kobayashi K, Tsukada M, Matsushige K, Yamada H (2013) Beyond the helix pitch: direct visualization of native DNA in aqueous solution. *ACS Nano* 7(2):1817–1822. doi:10.1021/nn400071n
3. Pyne A, Thompson R, Leung C, Roy D, Hoogenboom BW (2014) Singlemolecule reconstruction of oligonucleotide secondary structure by atomic force microscopy. *Small* 10(16):3257–3261. doi:10.1002/smll.201400265
4. Crampton N, Yokokawa M, Dryden DTF, Edwardson JM, Rao DN, Takeyasu K, Yoshimura SH, Henderson RM (2007) Fast-scan atomic force microscopy reveals that the type III restriction enzyme EcoP15I is capable of DNA translocation and looping. *Proc Natl Acad Sci U S A* 104(31):12755–12760. doi:10.1073/pnas.0700483104
5. Lyubchenko YL (2014) Nanoscale nucleosome dynamics assessed with timelapse AFM. *Biophys Rev* 6(2):181–190. doi:10.1007/s12551-013-0121-3
6. Miyagi A, Ando T, Lyubchenko YL (2011) Dynamics of nucleosomes assessed with time-lapse high-speed atomic force microscopy. *Biochemistry* 50(37):7901–7908. doi:10.1021/bi200946z
7. Adamcik J, Jeon J-H, Karczewski KJ, Metzler R, Dietler G (2012) Quantifying supercoiling-induced denaturation bubbles in DNA. *Soft Matter* 8(33):8651–8658. doi:10.1039/C2SM26089A
8. Fogg JM, Kolmakova N, Rees I, Magonov S, Hansma H, Perona JJ, Zechiedrich EL (2006) Exploring writhe in supercoiled minicircle DNA. *J Phys Condens Matter* 18(14):S145–S159. doi:10.1088/0953-8984/18/14/S01
9. Bussiek M (2003) Polylysine-coated mica can be used to observe systematic changes in the supercoiled DNA conformation by scanning force microscopy in solution. *Nucleic Acids Res* 31(22):137. doi:10.1093/nar/gng137
10. Li D, Lv B, Zhang H, Lee JY, Li T (2014) Positive supercoiling affiliated with nucleosome formation repairs non-B DNA structures. *Chem Commun* 50(73):10641–10644. doi:10.1039/C4CC04789C
11. Pyne ALB, Noy A, Main K, Velasco-Berrelleza V, Piperakis MM, Mitchenall LA, Cugliandolo FM, Beton JG, Stevenson CEM, Hoogenboom BW, Bates AD, Maxwell A, Harris SA (2019) Base-pair resolution analysis of the effect of supercoiling on DNA flexibility and recognition. *bioRxiv* 863423. doi:10.1101/863423
12. Klejevska B, Pyne ALB, Reynolds M, Shivalingam A, Thorogate R, Hoogenboom BW, Ying L, Vilar R (2016) Studies of G-quadruplexes formed within self-assembled DNA mini-circles. *Chem Commun* 52(84):12454–12457. doi:10.1039/c6cc07110d
13. Rothmund PW (2006) Folding DNA to create nanoscale shapes and patterns. *Nature* 440(7082):297–302. doi:10.1038/nature04586
14. Zhang P, Liu X, Liu P, Wang F, Ariyama H, Ando T, Lin J, Wang L, Hu J, Bin L, Fan C (2020) Capturing transient antibody conformations with DNA origami epitopes. *Nat Commun* 11:3114. doi:10.1038/s41467-020-16949-4
15. Dutta S, Rivetti C, Gassman NR, Young CG, Jones BT, Scarpinato K, Guthold M (2018) Analysis of single, cisplatin-induced DNA bends by atomic force microscopy and simulations. *Journal of Molecular Recognition* 31(10):e2731. doi:10.1002/jmr.2731
16. Cassina V, Seruggia D, Beretta G, Salerno D, Brogioli D, Manzini S, Zunino F, Mantegazza F (2011) Atomic force microscopy study of DNA conformation in the presence of drugs. *European Biophysics Journal* 40(1):59–68. doi:10.1007/s00249-010-0627-6
17. Osada E, Suzuki Y, Hidaka K, Ohno H, Sugiyama H, Endo M, Saito H (2014) Engineering RNA-protein complexes with different shapes for imaging and therapeutic applications. *ACS Nano* 8(8):8130–8140. doi:10.1021/nn502253c



18. Kundukad B, Cong P, van der Maarel JRC, Doyle PS (2013) Time-dependent bending rigidity and helical twist of DNA by rearrangement of bound HU protein. *Nucleic Acids Res* 41(17):8280–8288. doi:10.1093/nar/gkt593
19. Gaczynska M, Osmulski PA, Jiang Y, Lee J-K, Bermudez V, Hurwitz J (2004) Atomic force microscopic analysis of the binding of the *Schizosaccharomyces pombe* origin recognition complex and the spOrc4 protein with origin DNA. *Proc Natl Acad Sci U S A* 101(52):17952–17957. doi:10.2307/3374175
20. Heddle JG, Mittelheiser S, Maxwell A, Thomson NH (2004) Nucleotide binding to DNA gyrase causes loss of DNA wrap. *J Mol Biol* 337(3):597–610. doi:10.1016/j.jmb.2004.01.049
21. Katan AJ, Vlijm R, Lusser A, Dekker C (2015) Dynamics of nucleosomal structures measured by high-speed atomic force microscopy. *Small* 11(8):976–984. doi:10.1002/smll.201401318
22. Heenan PR, Wang X, Gooding AR, Cech TR, Perkins TT (2020) Bending and looping of long DNA by Polycomb repressive complex 2 revealed by AFM imaging in liquid. *Nucleic Acids Research* 48(6):2969–2981. doi:10.1093/nar/gkaa073
23. Hansma HG (2001) Surface biology of DNA by atomic force microscopy. *Annu Rev Phys Chem* 52(1):71–92. doi:10.1146/annurev.physchem.52.1.71
24. Mou J, Czajkowsky DM, Zhang Y, Shao Z (1995) High-resolution atomic-force microscopy of DNA: the pitch of the double helix. *FEBS Lett* 371(3):279–282. doi:10.1016/0014-5793(95)00906-P
25. Maaloum M, Beker A-F, Muller P (2011) Secondary structure of doublestranded DNA under stretching: elucidation of the stretched form. *Phys Rev E* 83(3):031903. doi:10.1103/PhysRevE.83.031903
26. Santos S, Barcons V, Christenson HK, Billingsley DJ, Bonass WA, Font J, Thomson NH (2013) Stability, resolution, and ultra-low wear amplitude modulation atomic force microscopy of DNA: small amplitude small set-point imaging. *Appl Phys Lett* 103(6):063702. doi:10.1063/1.4817906
27. Kominami H, Kobayashi K, Yamada H (2019) Molecular-scale visualization and surface charge density measurement of Z-DNA in aqueous solution. *Sci Rep* 9:6851. doi:10.1038/s41598-019-42394-5
28. Ares P, Fuentes-Perez ME, Herrero-Galan E, Valpuesta JM, Gil A, Gomez-Herrero J, Moreno-Herrero F (2016) High resolution atomic force microscopy of double-stranded RNA. *Nanoscale* 8:11818–11926. doi:10.1039/c5nr07445b
29. Lyubchenko YL, Shlyakhtenko LS (2009) AFM for analysis of structure and dynamics of DNA and protein–DNA complexes. *Methods* 47(3):206–213. doi:10.1016/j.ymeth.2008.09.002
30. Hansma HG, Laney DE (1996) DNA binding to mica correlates with cationic radius: assay by atomic force microscopy. *Biophys J* 70(4):1933–1939. doi:10.1016/S0006-3495(96)79757-6
31. Akpınar B, Haynes PJ, Bell NAW, Brunner K, Pyne ALB, Hoogenboom BW (2019) PEGylated surfaces for the study of DNA-protein interactions by atomic force microscopy. *Nanoscale* 11:20072–20080. doi:10.1039/C9NR07104K

# Materials

## Note

Prepare and store all reagents at  Room temperature , unless indicated otherwise.

## General Materials











1. 15-50 mL Falcon™ tubes.
2. Borosilicate glass bottle and volumetric flask (both 500 mL).
3. Eppendorf™ tubes, 0.5 and 2 mL, DNA and protein LoBind.
4. 6 mm mica substrates (Agar Scientific).
5. 15 mm magnetic stainless-steel discs (Agar Scientific).
6. Adhesive backed PTFE (Bytac® surface protection laminate).
7. Scalpel or punch.
8. Scotch™ tape.
9. Araldite® 2-part epoxy resin.
10. Stainless steel and plastic tip tweezers.
11. Petri dishes (35×10 mm).

## AFM Cantilevers

An appropriate cantilever should be chosen from the list below. The cantilever manufacturer, spring constant (N/m), resonant frequency in fluid (kHz, *see* **Note 1**) and nominal tip radius (nm) are provided.

1. FastScan-D (Bruker, 0.25 N/m, 110 kHz, 5 nm).
2. PEAKFORCE-HIRS-F-B (Bruker, 0.12 N/m, 30 kHz, 1 nm).
3. Biolever mini (Olympus, 0.1 N/m, 25 kHz, 10 nm).
4. MSNL-E (Bruker, 0.05 N/m, 7 kHz, 2 nm).

## Buffer Solutions

1. Ultrapure water (MilliQ®, resistivity > 18.2 MΩ (*see* **Note 2**).
2. Nickel adsorption and imaging buffer:  3 Millimolar (mM) NiCl<sub>2</sub> ,  20 Millimolar (mM) HEPES  7.4 , store on bench, ambient temperature. For 1 L, weigh out  4.76 g HEPES (molecular weight:  238.30 g/mol ) and  0.95 g NiCl<sub>2</sub> (molecular weight:  237.69 g/mol ).
3. Poly-L-lysine imaging buffer:  20 Millimolar (mM) HEPES  7.4 with or without  120 Millimolar (mM) NaCl , *see* **Note 3**. Used in methods both with and without copolymerisation with polyethylene glycol (PEG).

To prepare 500 mL of imaging buffer , carry out the following.

1. Gather a volumetric flask and borosilicate glass bottle (both 500 mL ), clean them by soaking and shaking in detergent (e.g. PCC-54™) and rinsing with ultrapure water until no bubbles remain (see **Note 2**).
2. Weigh out the necessary reagents with a cleaned spatula and dissolve in 200 mL ultrapure water in the bottle. Use a thoroughly cleaned magnetic stirrer to aid the dissolution process if required. The spatula and stirrer should be cleaned by rinsing with Ethanol, and ultrapure water and air-dried.
3. Pour into the volumetric flask and fill up just-below 500 mL with ultrapure water.
4. Pour back into the bottle. Check the pH of the solution using a well-calibrated and cleaned pH meter (three-point calibrated at pH 4, 7 and 10).
5. Adjust to the required pH using small amounts of concentrated (~ 1 Molarity (M) ) HCl or NaOH and a clean magnetic stirrer.
6. Pour into the volumetric flask and fill to the 500 mL mark with ultrapure water.
7. Filter the buffer by passage through a 0.2 µm syringe and store long-term in a glass bottle or short-term in a 15-50 mL Falcon™ tube.
8. Store buffers on the bench at Room temperature .
9. It is good practice to verify buffer cleanliness by imaging a freshly cleaved mica surface in the buffer: the mica should appear atomically flat and not show any noticeable contamination. If contamination is observed, the buffer can be filtered once more with a low kDa centrifugal spin column e.g. a 10 kDa cutoff centrifugal filter (Amicon Ultra, Millipore).

### DNA substrates

1. 339 base-pair DNA minicircles (store at 4 °C ) in 20 Millimolar (mM) HEPES pH 7.4 , at a concentration of ~ 10 ng/µl (see **Note 4**).
2. 496 base-pair linear DNA (store at 4 °C ) in 10 Millimolar (mM) HEPES pH 7.8 at concentrations between 1.5 ng/µl and 20 ng/µl (see **Note 4**).

### Safety warnings

! For hazard information and safety warnings, please refer to the SDS (Safety Data Sheet).

### Before start

Prepare Buffer Solutions as described in section '**Materials**'.

## Attachments



Imaging\_DNA  
\_by\_AFM\_P...

2.5MB

## Files

 SEARCH

### Protocol



NAME

#### 1 Preparation of Mica Substrate

VERSION 1

CREATED BY



**Alice L Pyne**

Department of Materials Science, Sir Robert Hadfield Building, University of Sheffield, S1 3JD

OPEN →

### Protocol



NAME

#### 2 Methods for DNA Adsorption on a Mica Substrate for AFM Imaging in Fluid

VERSION 1

CREATED BY



**Alice L Pyne**

Department of Materials Science, Sir Robert Hadfield Building, University of Sheffield, S1 3JD

OPEN →

### Protocol



NAME

#### 3 Pre-imaging Setup for High Resolution AFM in Fluid

VERSION 1

CREATED BY



**Alice L Pyne**

Department of Materials Science, Sir Robert Hadfield Building, University of Sheffield, S1 3JD

OPEN →

### Protocol



NAME

#### 4 Optimizing AFM Imaging in PFT for High Resolution AFM Imaging on DNA

VERSION 1

CREATED BY

**Alice L Pyne**





Department of Materials Science, Sir Robert Hadfield Building, University of Sheffield, S1 3JD

**OPEN** →

## Protocol



NAME

**5 Methods for DNA-protein imaging by AFM in fluid**

VERSION 1

CREATED BY



**Alice L Pyne**

Department of Materials Science, Sir Robert Hadfield Building, University of Sheffield, S1 3JD

**OPEN** →